Low Cost Development of a Nonlinear Simulation for a Flexible Uninhabited Air Vehicle

Aditya Kotikalpudi, Claudia Moreno, Brian Taylor, Harald Pfifer and Gary Balas[1]

***Abstract*— The development of a nonlinear simulation environment for an uninhabited air vehicle with a flexible airframe is presented. Simple, yet efficient testing procedures are employed to estimate the physical properties of the aircraft. The aerodynamic forces and moments are obtained using a doublet lattice method. The interaction between structural dynamics and aerodynamics is given special attention from a modeling standpoint. The simulation is finally integrated into the existing simulation infrastructure maintained by the research group. A modular approach is emphasized in the simulation build-up, which allows for easy switching between models.**

I. INTRODUCTION

The University of Minnesota (UMN) uninhabited air vehicle (UAV) research group [1] has developed multiple low cost testbeds based on Ultra Stick 25e UAV along with their simulations and testing infrastructure such as software and hardware-in-the-loop testing and flight test data analysis capabilities [2]. A number of research areas are being studied with this fleet ranging from guidance and navigation to fault detections [3], [4]. The simulations of these testbeds are publicly available for download from the laboratory website (`uav.aem.umn.edu`) to encourage the aerospace community to engage in the research efforts in this field.

There has been a growing need for such low cost, open source testbeds for research in the field of aeroservoelasticity, which is an ongoing research area within the group. The current fleet of testbeds does not fulfill this requirement since the aircraft have a very rigid airframe. Hence, the design and construction of a new platform, denoted mini-MUTT (Multi-Utility Technology Testbed), is being pursued. The design is based on the body freedom flutter (BFF) vehicle, which has been developed by the Air Force Research Laboratory (AFRL) in cooperation with Lockheed Martin (LM) [5]. AFRL and LM have generously donated one BFF vehicle to the UMN UAV research group. A design drawing of the mini-MUTT is shown in Fig. 1.

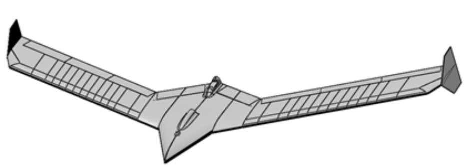

Fig. 1. Model of mini-MUTT aircraft

[1]A. Kotikalpudi, C. Moreno, B. Taylor, H. Pfifer and G. Balas are with the Aerospace Engineering and Mechanics Department, University of Minnesota, emails: kotik001@umn.edu, moren148@umn.edu, brtaylor@umn.edu, hpfifer@umn.edu, balas@aem.umn.edu

In contrast to the BFF aircraft, the mini-MUTT will feature a modular design consisting of a common center body and interchangeable wings with progressively increasing flexibility. The modular approach is based on Lockheed Martin's X-56A MUTT design [6], which is being pursued for synthesis of flutter suppression and gust load alleviation control algorithms. The UMN UAV research group intends to use its own fleet of mini-MUTTs and their simulations to gain insights into aeroservoelastic systems via efficient modeling techniques, robustness analysis and model validation through flight tests. These insights will be applicable in tasks like model order reduction and sensor/actuator selection for control law synthesis.

As an initial step, a center body with a set of rigid wings has been constructed, with emphasis on achieving the rigid body mass properties as close to the BFF aircraft as possible (Fig. 2.

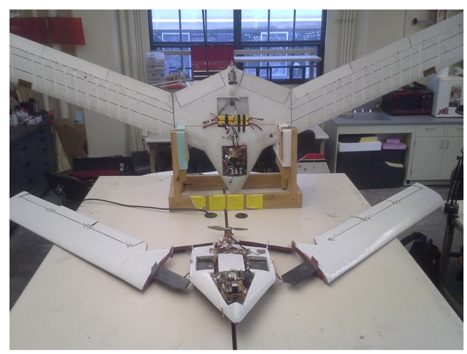

Fig. 2. The mini-MUTT aircraft with BFF aircraft in background

The same open source philosophy that is a trademark of the research conducted by the UMN UAV group will be followed in the mini-MUTT project. Raw data and detailed reports of all experiments and computational analysis presented in this paper will be published on the group website `uav.aem.umn.edu`.

This paper presents the procedures used to develop a nonlinear simulation for a flexible aircraft. It has been implemented for the BFF aircraft and will eventually be used to simulate the fleet of mini-MUTTs. Section II provides a comprehensive literature review on the various methodologies used to model aeroelastic systems, followed by a description of the subsystem based approach adopted to construct this simulation in section III. A combination of ground tests on the BFF aircraft to obtain mass properties [7], [8] and computational aerodynamics analysis [9], see section IV, have been performed. The data from the experiments and analysis is integrated into the nonlinear simulation framework of the UMN UAV research group [2], see section V. A linear analysis is done for a preliminary flutter analysis where the airspeeds corresponding to onset of various flutter modes are identified.

II. Literature Review

Aeroservoelasticity is a phenomenon where the structural dynamics of an aircraft with a flexible airframe interacts with the aerodynamic loads generated during flight, and the flight control law [10], [11]. The multidisciplinary nature of this field requires researchers to integrate principles of aerodynamics, structural dynamics, rigid body flight dynamics and control design. In order to gain insights into such systems and synthesize active flutter suppression control algorithms for them, accurate and efficient models of the aircraft need to be developed.

The advent of potential flow based panel methods for aerodynamics [12], [13], [14] and finite element modeling for structural analysis [15], [16] in the 1960s and 1970s led to detailed modeling capabilities of complex aircraft geometries. Since then, many different methodologies have been used to model aeroelastic phenomena for aircraft [17], [18]. These methodologies mainly differ on the account of their underlying modeling assumptions for aerodynamics and structural dynamics such as

- *Steady vs. unsteady flow*: an unsteady flow condition assumes the fluid flow properties at any given point in the system to vary with time [19], which is typically the case for phenomena like flutter. Hence, the flow is often assumed unsteady for modeling aeroelastic systems [20], [21], [22]. However, in order to simplify modeling procedures, the steady flow conditions can be enforced by assuming a quasi-steady fluid flow in order to model flutter [23], [24].
- *Linear vs nonlinear structural model*: a linear structural model is considered sufficient to model small deflections while a nonlinear structural model is required to model nonlinear effects like bilinear stiffness (due to loosely connected structural components) or geometric nonlinearities (due to large deflections) [24], [25].

Modeling of aerodynamics and structural dynamics also depends on the manner in which they are integrated into the combined aeroelastic model. For instance, the aerodynamic model could be constructed in parallel with the structural model, ensuring that the discretization of the aircraft in both models match one to one, i.e. for every node in the finite element structural model, there is a corresponding panel in the aerodynamic model and vice versa [20], [24], [26]. This allows for a relatively easy way to construct numerical simulations for the overall aeroelastic model. Alternatively, the aerodynamic and structural model can be developed independently, invariably resulting in differences in their grids [21], [27], [28]. Hence the aero-structural interconnections include an interface which interpolates between the two grids. This modular approach, although more complicated, is very useful since it helps retain the ability to work with the aerodynamic and structural model independently of one another.

III. SUBSYSTEM BASED SIMULATION ARCHITECTURE

The approach to aeroelastic system modeling described in this paper is based on the philosophy of a subsystem based simulation architecture, where the aerodynamic and structural models are developed and kept separate. The interconnections between them have suitable transformation matrices which interpolate between the aerodynamic model grid points and the nodes of the finite element based structural model, see section IV. Conceptually, the aero-structural interaction can be thought of as an interconnection as shown in Fig. 3.

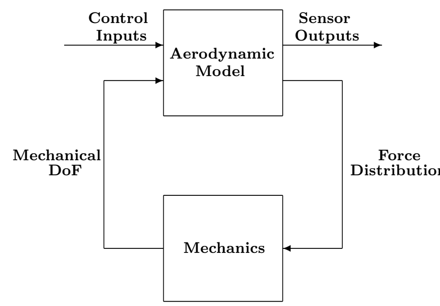

Fig. 3. Aerodynamic and structural model interaction

The mechanics block in Fig. 3 generally represents all the mechanical degrees of freedom of an aircraft, i.e. the rigid body and structural vibration modes. It should be noted that this methodology accommodates any assumption made for the aerodynamic and structural models (i.e. steady/unsteady flow or linear/nonlinear structural dynamics).

The aeroelastic model represented in Fig. 3 can be considered analogous to a linear fractional transformation (LFT) [29]. This characteristic is one of the main reasons behind choosing this architecture. The LFT interconnection is a standard tool for multivariable control and robustness analysis. Another advantage of this architecture is that uncertainty analysis or order reduction of subsystems can be done individually [30], [31]. It also allows for insights on the effects of individual subsystem fidelity on overall model accuracy. Finally, it is easier to switch between different aerodynamic or structural models for a given aircraft. Hence, this architecture can handle the mini-MUTT fleet very efficiently.

IV. STRUCTURAL AND AERODYNAMIC MODELS

Tests were conducted on the BFF aircraft to determine its structural properties. The structural model is assumed to be linear since the deflections in flight are expected to have a small amplitude. An unsteady aerodynamic model has been developed by the Institute of System Dynamics and Control of the German Aerospace Center (DLR), which employs a doublet lattice method (DLM) based on potential flow.

A. Mass Properties

Estimates of the moments of inertia and center of gravity of the aircraft were obtained from experiments. For all the tests, the aircraft was assumed to be perfectly symmetric along the xz- and xy-plane, which is a standard assumption for aircraft. The estimated values are reported in Table I.

TABLE I
MASS PROPERTIES

Property	Value
Total mass	5.42 kg
CG location	0.59 m (from nose)
Pitching moment of inertia	0.36 $kg - m^2$
Rolling moment of inertia	2.50 $kg - m^2$
Yawing moment of inertia	2.37 $kg - m^2$

1) Center of Gravity: the center of gravity (CG) of the aircraft was located using three weighing scales, one under each winglet and the third under the center keel (Fig. 4).

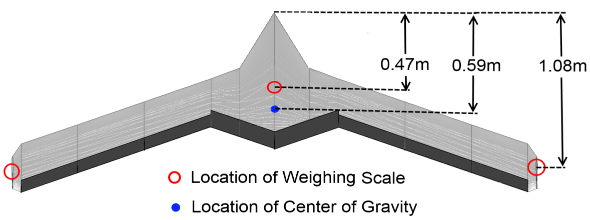

Fig. 4. Center of Gravity testing for BFF aircraft

The readings from the three scales were used to determine the longitudinal coordinate of CG using equation (1).

$$\bar{x} = \frac{m_{aft}x_{aft} + m_{fore}x_{fore}}{m_{tot}} \quad (1)$$

where $\bar{x}$ is the longitudinal coordinate of CG, m_{aft} is the sum of the readings of the scales under the winglets, m_{fore} is the reading of the scale under the center keel, x_{aft} is the location of the scales under the winglets with respect to the nose of the aircraft, x_{fore} is the location of the scale under the center keel and m_{tot} is the sum of the readings of all the scales (Table I).

2) Moments of Inertia: the principal moments of inertia of the aircraft (I_{xx}, I_{yy} and I_{zz}) were determined via swing tests. The coupling terms of the inertia tensor (I_{xz}, I_{xy}, I_{yz}) were assumed to be zero. For the latter two, this assumption is justified by the symmetry considerations. I_{xz} can be considered zero since the aircraft lacks a large vertical fin. While the pitch moment of inertia was determined using a compound pendulum approximation (Fig. 6), the roll and yaw moments of inertia were determined using a bifilar pendulum approach (Fig. 5) [32]. Keeping infrastructural limitations in mind, reasonable assumptions and simplifications were made to extract the data in a simple cost-effective manner. The primary assumption was small deflections of the aircraft during these swing tests, to allow the usage of linear approximations of the physical systems. Equations (2) and (3) describe the linear approximations of dynamics of the compound pendulum and bifilar pendulum respectively [33].

$$I = \frac{mgd}{\omega^2} \quad (2)$$

$$I = \frac{mgd^2}{4L\omega^2} \quad (3)$$

I is the moment of inertia of the body, m is the mass of the body, g is acceleration due to gravity and ω is the frequency of oscillations. In equation (3), L is the length of the two filars and d is the horizontal distance between them (Fig. 5).

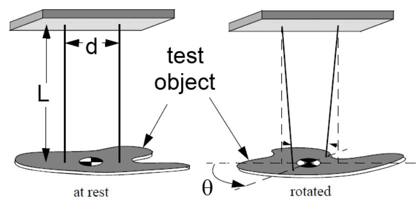

Fig. 5. Schematic diagram of a bifilar pendulum [7]

Fig. 6. Inertia swing setup for pitch moment of inertia

3) Finite Element Model: The finite element model has been constructed using Euler beam elements which have three degrees of freedom (DoF) - translation, transverse bending and twist along longitudinal axis. Discretization of the aircraft into these elements is mainly based on the physical locations of components such as winglets, actuators and other electronics. Fig. 7 shows the finite element model for the BFF aircraft.

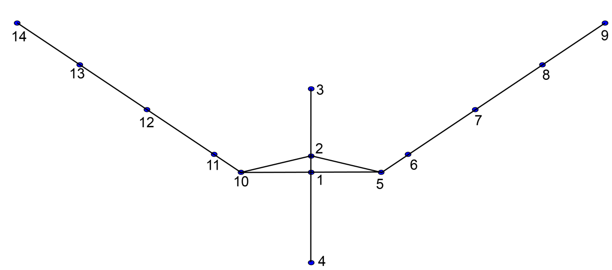

Fig. 7. Finite Element Model for the BFF Aircraft

The model has a total of 14 nodes, resulting in 42 DoF overall (3 DoF per node). These DoF are decoupled via modal decomposition [34] which transforms the system into modal coordinates. The center body is assumed rigid and therefore the beam elements representing it (nodes 1-5 and 10) have very high stiffness. The boundary conditions for the model are are assumed to be free-free. This results in the rigid modes of the aircraft showing up at very low frequencies due to numerical errors in the model. These modes are truncated, as are the high frequency modes [8]. A total of 12 flexible modes are retained in the structural model, represented by equation (4).

$$M_f \ddot{\eta}(t) + B_f \dot{\eta}(t) + K_f \eta(t) = F_{modal}(t) \tag{4}$$

M_f, B_f and K_f are the modal mass, damping and stiffness matrices respectively, all obtained from the finite element model. F_{modal} is the modal forces matrix and η is the modal coordinates vector. The truncated rigid modes are replaced by nonlinear rigid equations of motion when the simulation is constructed, see section V. Both static and dynamic experiments have been performed to obtain the mass and stiffness properties of the vehicle. In addition, a ground vibration test has been performed to update the FEM model [8].

B. Aerodynamic Model

An unsteady aerodynamic model of the aircraft has been developed by the DLR [21] based on the DLM [9]. The DLM gives a harmonic solution to the unsteady Prandl-Glauert equation in the frequency domain for a lifting surface oscillating at a constant frequency. The aerodynamic model has been constructed by discretizing the aircraft geometry into 1664 panels and applying the DLM to solve for the generalized aerodynamic force matrix Q. This matrix maps the structural displacements to the aerodynamic forces by

$$F_{aero} = \bar{q} S Q(\tilde{\omega}) \eta \tag{5}$$

In equation 5, $\bar{q}$ is the dynamic pressure, S a matrix giving the panel areas and η the structural displacements as given in Equation 4. The generalized aerodynamic force matrix Q is a function of the reduced frequency $om\tilde{e}ga = \frac{c}{2U_\infty}$, where c is the mean aerodynamic chord, U_∞ the free-stream velocity. Note that it is implicitly assumed in Equation 5 that Q has been transformed in the modal domain. This ensures compatibility with the structural model which is also given in the modal domain. Since different grids are used to model the structural dynamics and the aerodynamics, a coordinate transformation T_{sa} has to be performed to get from the aerodynamic loads F_{aero} to the structural loads F_{modal}.

$$F_{modal} = \bar{q} T_{sa} S Q(\tilde{\omega}) \eta \tag{6}$$

It should be noted that the reverse transformation of T_{sa} is included in Q to transform displacements on the structural grid to displacements on the aerodynamic grid. Also, for simplification the control surface deflections are not considered in Equations 5 and 6. It is straightforward to obtain an extended Q that also maps the control surface deflections to the aerodynamic forces [21].

Finally, since $Q(\tilde{\omega})$ can only be calculated at discrete frequencies, a rational function approximation (RFA) [35], [21] is applied to obtain an aerodynamic model for time domain calculations. The procedure is to calculate $Q(\tilde{(\omega)})$ at different frequencies and the obtained data is fitted to a rational function in the Laplace domain, using least squares method. The rational function is given by

$$Q(s) = Q_0 + Q_1 s + Q_2 s + \sum_{l=1}^{n} Q_{l+2} \frac{s}{s + b_l} \tag{7}$$

where Q_0 is a quasi-steady term, Q_1 is the added mass term and Q_2 is the acceleration term. The Q_{l+2} term takes into account the lag behavior of unsteady flow. The poles of these lag terms are chosen by the user.

C. Aero-Structural Grid Interpolation

In order to map the displacements from the structural grid on to the aerodynamic grid and also calculate the modal forces for the structural grid from the aerodynamic force distribution, a transformation matrix T_{sa} (equation **??**) is calculated. It should be noted that the structural model grid is the set of coordinates locating the nodes in the finite element model, while the aerodynamic grid is the set of coordinates locating the center points of the panels in the aerodynamic model.

T_{sa} matrix is calculated by first constructing a spline grid as shown in Fig. 8.

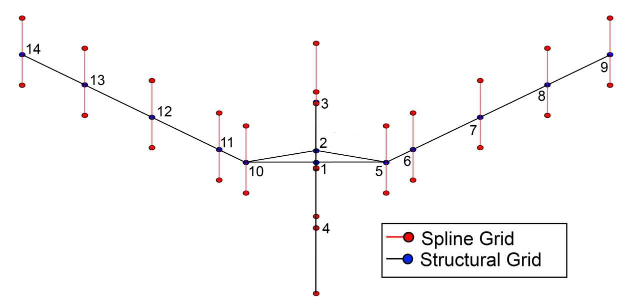

Fig. 8. Spline Grid Layout

Each of the red connections of the spline grid is assumed to be stiff. It is assumed to be attached to an infinite plate and move in a rigid manner along with the structural grid. A radial basis function [36], [37] is then used to calculate displacements at the locations on the infinite plate specified by the aerodynamics grid, based on displacements of the spline grid.

V. NONLINEAR SIMULATION

The UMN UAV Research Group maintains a simulation environment of its aircraft [1]. The architecture of the simulation is modular which allows for switching between different aircraft within the same framework. The simulation for the BFF aircraft has been built upon this existing infrastructure, thereby enhancing its capability to simulate the rigid and flexible body dynamics of an aircraft. The aero-structural interconnection described in section IV is employed to achieve this. The rigid dynamics are added to the aeroelastic model using the standard 6 DoF equations of motion.

A. Integration of Nonlinear Rigid Dynamics

The mechanics block shown in Fig. 3 represents both, the rigid and the flexible dynamics of the aircraft. In order to represent the rigid modes with nonlinear equations while keeping the flexible modes linear using the linear finite element model, the rigid modes are separated from the flexible modes. This separation is possible if the mean axes of the aircraft are chosen as the body fixed axes [26]. A schematic representation of this division is shown in Fig. 9.

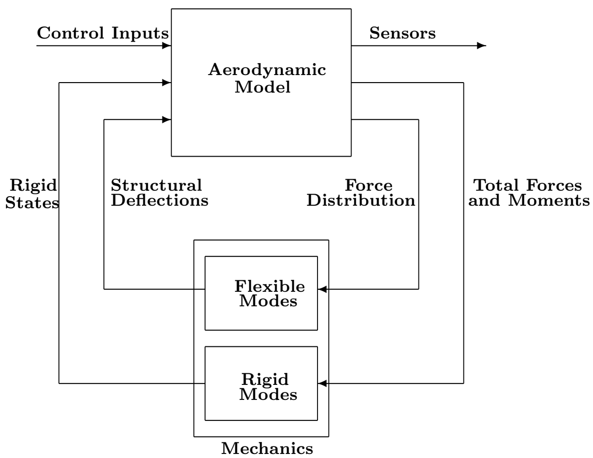

Fig. 9. Aerodynamic and structural dynamics interconnection

The rigid body dynamics are represented using the standard 6 DoF equations of motion, as given by equation (8)

$$\begin{bmatrix} m(\dot{V}_r + \Omega_r \times V_r - T_g g) \\ I_r \dot{\Omega}_r \times I_r \Omega_r \end{bmatrix} = F_r(t) \tag{8}$$

m and I_r are the aircraft mass and moments of inertia, V_r and Ω_r are the rectilinear and angular velocities along the body fixed axes, T_g is the rotation matrix from inertial axes to the body fixed axes for gravity and F_r is the set of body forces and moments. The rigid modes are transformed into modal coordinates via a set of pseudo modal vectors, generated by noting displacements of the nodes in the finite element model for unitary rigid mode displacements. Since the aerodynamic model and the flexible modes are also in modal coordinates (equations (6), (4)), the aero-structural interconnection (Fig. 9) is achieved smoothly.

B. Simulation Results

Software and hardware-in-the-loop testing facilities and, trimming and linearization functions of the nonlinear model have been developed as a part of the simulation framework [1]. These tools can be used to generate linear models of the aircraft are specific flight conditions. It is ensured that the flexible aircraft simulation is compatible with these functionalities. A linear analysis has been carried out to look for the airspeeds at which the flutter modes become unstable. Table II compare this data with the data published by Lockheed Martin [5].

TABLE II
MASS PROPERTIES

Flutter Modes		UMN	Lockheed
Body Freedom Flutter	Pole	$0.833 \pm 27.2i$	$1.66 \pm 24.3i$
	Freq	4.32 Hz	3.88 Hz
	Velocity	24 m/s	22.62 m/s
Sym Bending/torsion	Pole	$0.157 \pm 59.5i$	$2.01 \pm 62.38i$
	Freq	9.51 Hz	9.93 Hz
	Velocity	31 m/s	30.84 m/s
A/S Bending/Torsion	Pole	$4.52 \pm 55.6i$	$1.66 \pm 67.06i$
	Freq	8.85 Hz	10.68 Hz
	Velocity	35 m/s	31.86 m/s

Table II shows that the airspeed at which the body freedom flutter mode goes unstable is reasonably accurate, although the predicted frequency and damping of the mode is different from that of LM data. It is hoped that validation through flight test data in the near future should help remove these minor differences.

Fig. 10 and 11 show the frequency responses of the linear model at the flight conditions listed in table II.

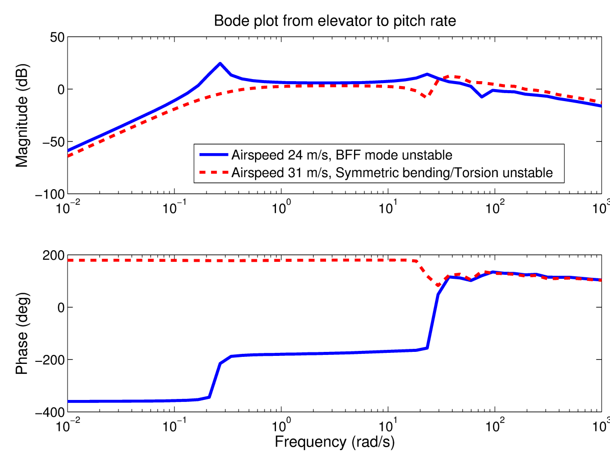

Fig. 10. Bode plots at flutter points - Longitudinal dynamics

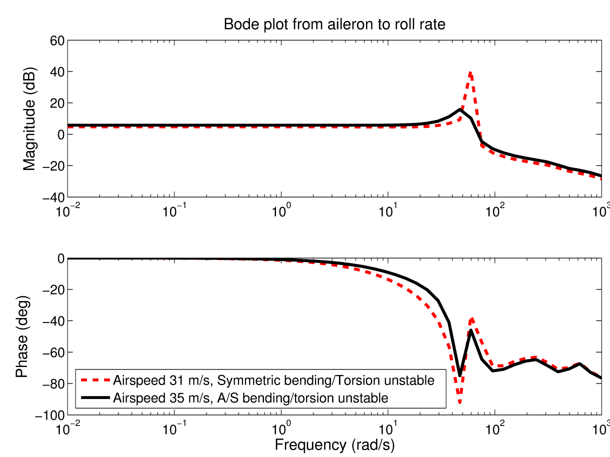

Fig. 11. Bode plots at flutter points - Lateral-directional dynamics

CONCLUSION

A nonlinear simulation of a flexible aircraft has been developed and has been implemented within the simulation framework already developed in the laboratory [2]. A procedure for developing such simulations has been established, which uses simple analysis tools and testing procedures. In due course of time, the simulation will be updated with data from the first mini-MUTT, which would be publicly available for download from the laboratory website. Multiple aircraft with varying flexibility will be constructed and simulations will be built using the same procedures.

The subsystem approach used to model these systems will also be employed for tasks like model order reduction and subsystem error analysis. As mentioned earlier, these testbeds and their simulations will give significant insights into the interactions between various subsystems as well as the overall behavior of aeroservoelastic systems. It is hoped that the aerospace community will take advantage of the testbeds to design and test their flutter suppression or gust load alleviation control algorithms and contribute to the research efforts in this field.

ACKNOWLEDGMENT

This work was supported by NASA contract number NNXIIC109P entitled 'Robust Aeroservoelastic Control Utilizing Physics Based Aerodynamic Sensing' as a subcontract to Tao systems. Dr Arun Mangalam is the principal investigator and Dr Martin Brenner is the NASA technical monitor.

REFERENCES

[1] B. Taylor, A. Dorobantu, and G. Balas, "University of minnesota uav research group," *Online at: www. uav. aem. umn. edu*.

[2] A. Dorobantu, W. Johnson, F. A. Lie, B. Taylor, A. Murch, Y. C. Paw, D. Gebre-Egziabher, and G. Balas, "An airborne experimental test platform: From theory to flight," in *American Control Conference*, 2013, pp. 659–673.

[3] A. Dorobantu, A. Murch, B. Mettler, and G. Balas, "Frequency domain system identification for a small, low-cost, fixed-wing uav," in *AIAA Guidance, Navigation, and Control Conference*, 2011.

[4] R. Pandita, "Dynamic flight envelope assessment with flight safety applications," Ph.D. dissertation, University of Minnesota, 2010.

[5] E. Burnett, C. Atkinson, J. Beranek, B. Sibbitt, B. Holm-Hansen, and L. Nicolai, "Ndof simulation model for flight control development with flight test correlation," in *AIAA Modeling and Simulation Technologies Conference*, vol. 3, 2010, pp. 7780–7794.

[6] G. Creech, "Introducing the x-56a mutt: Who let the dog out?" *Online at:* $www.nasa.gov/topics/aeronautics/features/x-56a\_mutt.html$.

[7] M. R. Jardin and E. R. Mueller, "Optimized measurements of uav mass moment of inertia with a bifilar pendulum," in *AIAA Guidance, Navigation and Control Conference, SC, USA*, 2007.

[8] C. Moreno, A. Gupta, B. Taylor, H. Pfifer, and G. J. Balas, "Identification of a structural model for a highly flexible aircraft," in *American Control Conference*, 2014, accepted.

[9] E. Albano and W. P. Rodden, "A doublet-lattice method for calculating lift distributions on oscillating surfaces in subsonic flows." *AIAA journal*, vol. 7, no. 2, pp. 279–285, 1969.

[10] D. Cox, H. Curtiss Jr, J. Edwards, K. Hall, D. A. Peters, R. Scanlan, E. Simiu, and F. Sisto, *A modern course in aeroelasticity*. Springer, 2006, vol. 116.

[11] Y. C. Fung, *An introduction to the theory of aeroelasticity*. Courier Dover Publications, 2002.

[12] S. M. Belotserkovskii, "Study of the unsteady aerodynamics of lifting surfaces using the computer," *Annual Review of Fluid Mechanics*, vol. 9, no. 1, pp. 469–494, 1977.

[13] G. R. Hough, "Remarks on vortex lattice methods." *Journal of Aircraft*, vol. 10, no. 5, pp. 314–317, 1973.

[14] C. E. Lan, "A quasi-vortex lattice method in thin wing theory," *Journal of Aircraft*, vol. 11, no. 9, pp. 518–527, 1974.

[15] R. W. Clough and J. L. Tocher, "Finite element stiffness matrices for analysis of plates in bending," in *Proceedings of conference on matrix methods in structural analysis*, vol. 1, 1965.

[16] D. Ngo and A. Scordelis, "Finite element analysis of reinforced concrete beams," in *American Concrete Institute Journal Proceedings*, vol. 64, no. 3, 1967.

[17] P. P. Friedmann, "Renaissance of aeroelasticity and its future," *Journal of Aircraft*, vol. 36, no. 1, pp. 105–121, 1999.

[18] E. Livne, "Future of airplane aeroelasticity," *Journal of Aircraft*, vol. 40, no. 6, pp. 1066–1092, 2003.

[19] J. Katz and A. Plotkin, *Low speed aerodynamics: From wing theory to panel methods*. New York: Mc–Graw-H ill Book Co, 1991.

[20] M. J. Patil, D. H. Hodges, and C. E. S. Cesnik, "Nonlinear aeroelasticity and flight dynamics of high-altitude long-endurance aircraft," *Journal of Aircraft*, vol. 38, no. 1, pp. 88–94, 2001.

[21] T. Kier and G. Looye, "Unifying manoeuvre and gust loads analysis models," *International Forum on Aeroelasticity & Structural Dynamics*, 2009.

[22] E. H. Dowell and D. Tang, "Nonlinear aeroelasticity and unsteady aerodynamics," *AIAA journal*, vol. 40, no. 9, pp. 1697–1707, 2002.

[23] M. R. Waszak, "Modeling the benchmark active control technology wind-tunnel model for application to flutter suppression," in *AIAA Atmospheric Flight Mechanics Conference, San Diego, California*, vol. 96, no. Paper No. 96-3437, 1996.

[24] C. M. Shearer and C. E. Cesnik, "Nonlinear flight dynamics of very flexible aircraft," *Journal of Aircraft*, vol. 44, no. 5, pp. 1528–1545, 2007.

[25] M. J. Patil and D. H. Hodges, "On the importance of aerodynamic and structural geometrical nonlinearities in aeroelastic behavior of high aspect-ratio wings," *Journal of Fluids and Structures*, vol. 19, no. 7, pp. 905–915, 2004.

[26] M. R. Waszak and D. K. Schmidt, "Flight dynamics of aeroelastic vehicles," *Journal of Aircraft*, vol. 25, no. 6, pp. 563–571, 1988.

[27] S. A. Morton, B. Tillman, D. R. McDaniel, D. R. Sears, and T. R. Tuckey, "Kestrel- a fixed wing virtual aircraft product of the create program," in *Department of Defense High Performance Computing Modernization Program Users Group Conference*. IEEE, 2009, pp. 148–152.

[28] C. Farhat, M. Lesoinne, and P. Le Tallec, "Load and motion transfer algorithms for fluid/structure interaction problems with non-matching discrete interfaces: momentum and energy conservation, optimal discretization and application to aeroelasticity," *Computer methods in applied mechanics and engineering*, vol. 157, no. 1, pp. 95–114, 1998.

[29] S. Skogestad and I. Postlethwaite, *Multivariable feedback control: analysis and design*. Wiley New York, 2007, vol. 2.

[30] A. Varga and B. Anderson, "Accuracy-enhancing methods for balancing related frequency-weighted model and controller reduction," *Automatica*, vol. 39, no. 5, pp. 919–927, 2003.

[31] B. Anderson and Y. Liu, "Controller reduction: concepts and approaches," *IEEE Transactions on Automatic Control*, vol. 34, no. 8, pp. 802–812, 1989.

[32] C. Schedlinski and M. Link, "A survey of current inertia parameter identification methods," *Mechanical systems and signal processing*, vol. 15, no. 1, pp. 189–211, 2001.

[33] G. R. Fowles and G. L. Cassiday, *Analytical mechanics*. Saunders College, 1999.

[34] A. Dimarogonas, *Vibration for Engineers. 1996*. Prentice-Hall International Editions.

[35] K. L. Roger, "Airplane math modeling methods for active control design," *Advisory Group for Aerospace Research and Development CP-228*, pp. 4–1, 1977.

[36] M. D. Buhmann, *Radial basis functions: theory and implementations*. Cambridge University Press, 2003, vol. 12.

[37] W. P. Rodden and E. H. Johnson, *MSC/NASTRAN Aeroelastic Analysis: User's Guide, Version 68*. MacNeal-Schwendler Corporation, 1994.